



Optical Characterization of Atmospheric Aerosols via Airborne Spectral Imaging and Self-Organizing Map for Climate Change Diagnostics

John W. Makokha*, Jared O. Odhiambo

Department of Science Technology and Engineering, Kibabii University, Bungoma, Kenya

Email: *makokhajw@kibu.ac.ke

How to cite this paper: Makokha, J.W. and Odhiambo, J.O. (2018) Optical Characterization of Atmospheric Aerosols via Airborne Spectral Imaging and Self-Organizing Map for Climate Change Diagnostics. *Open Access Library Journal*, 5: e4698. <https://doi.org/10.4236/oalib.1104698>

Received: May 31, 2018

Accepted: August 20, 2018

Published: August 23, 2018

Copyright © 2018 by authors and Open Access Library Inc.

This work is licensed under the Creative Commons Attribution International License (CC BY 4.0).

<http://creativecommons.org/licenses/by/4.0/>



Open Access

Abstract

Self-Organizing Map (SOM) analysis is used to perform optical characterization of both Aerosol Optical Depth (AOD) and Ångström Exponent (ÅE) retrieved from Moderate-resolution Imaging Spectroradiometer (MODIS) in relation to Precipitation Rate (PR) from Tropical Rainfall Measurement Mission (TRMM) over selected East African sites from 2000 to 2014 and further diagnose climate change over the region if any. SOM reveals a marked spatial variability in AOD and ÅE that is associated to changing aerosol transport, urban heat islands, diffusion, direct emission, hygroscopic growth and their scavenging from the atmosphere specific to each site. Temporally, all sites except Mbita and Kampala indicate two clusters in AOD that are associated to prevailing dry and wet seasons over East Africa. Moreover, all sites except Mbita and Mount Kilimanjaro show two clusters in ÅE that are related to aerosol mode of generation and composition over the region. The single cluster in AOD and ÅE over Mbita indicate that aerosol characteristics over the site are influenced by biomass burning and local air circulation rather than the monsoon precipitation throughout the study period.

Subject Areas

Atmospheric Sciences, Environmental Sciences, Geophysics

Keywords

Aerosol Optical Depth, Self-Organizing Map, Ångström Exponent, Neural Network, Remote Sensing, East African Atmosphere

1. Introduction

Utilization of univariate techniques in optical characterization of atmospheric aerosols increases the likelihood of an observation occurring by chance (false-positive results) [1]. With this in mind, a number of studies have illustrated the possibility of utilizing the multivariate techniques among them Principle Component Analysis (PCA) in aerosol characterization [2]. In this study, PCA investigations quantified the influence of rainy and dry spells on aerosol characteristics over the region. In the quest to further understand factors that significantly influence aerosol variability and further project their future characteristics, it is necessary to use techniques with capabilities of extracting aerosol properties and characteristic patterns of variability within a large spectral data that is currently available.

Monitoring of atmospheric processes in relation to climate change require pattern detection techniques such as Self Organizing Map (SOM) that effectively cluster, classify and perform future extraction in multispectral data sets [3] [4]. SOM has been utilized in Aerosol Optical Depth (AOD) and Precipitation Rate (PR) projections over east Africa as detailed in [5]. As a tool for pattern recognition and classification, the SOM analysis is in widespread use across a number of disciplines among the climate research [6] [7] [8] [9] [10]. The current study explores the utilization of SOM as a novel technique in the optical characterization of atmospheric aerosols for climate change diagnostics over the region.

Airborne spectroscopic measurements from MODIS that necessitates the retrieval of both AOD and ÅE are on board the Earth Observing System (EOS) namely, Terra satellite operating at an altitude of 705 km [11] [12] was utilized. The MODIS TERRA (EOS AM-1) was launched on December 18, 1999 and passes the Equator at 10:30am daily (descending mode). MODIS images simultaneously both reflected solar radiance and terrestrial emission in 36 channels (0.41 - 14.4 μm wavelength range) with resolutions varying between 0.25 - 1 km [13]. On the other hand, PR retrieved from TRMM that is jointly supported by NASA and Japan's National Space Development Agency space missions to basically monitor and study tropical and subtropical precipitation. The mission started in November 1997 at an altitude of about 402.5 km with its orbit ranging between 35° north and 35° south of the equator which allows it to cover the entire Earth daily [14].

It is important to note that SOM technique can be utilized through its respective MATLAB toolbox that is available free online. The SOM MATLAB Toolbox (version 2.0) uses MATLAB structures, making it convenient to tailor the code for specific user needs and can be downloaded from a Website of the Helsinki University of Technology, Finland: <http://www.cis.hut.fi/projects/somtoolbox/>.

2. Methodology

2.1. Description of Study Area and Spectral Data Manipulation

The East Africa region covers diverse land forms comprising of glaciated moun-

tains, Semi-Arid, Plateau and Coastal regions. Details and the map illustrating the study region and specifics over each site of study are as shown in [15].

Level-3 MODIS gridded atmosphere monthly global product “MOD08_M3” at spatial resolution of $1^\circ \times 1^\circ$, was used in the current study for optical characterization of AOD (at 550 nm) and Ångström Exponent (ÅE) (at 470 - 660 nm) in relation to Precipitation Rate (PR) over selected sites of East Africa from 2000 to 2014. MODIS level 3 monthly data was rearranged in a 2D array with the rows and columns representing the temporal and spatial dimensions respectively. The row vector at each time step was used to update the weight of the SOM via an unsupervised learning algorithm. The outcome weight vectors of the SOM nodes are reshaped back into characteristic data patterns [4] [6].

2.2. Self-Organizing Map and Its Training Rules

SOM has the capability of simultaneously affording, clustering, classifying and feature extraction of a multidimensional nonlinear spectroscopic data [5] [16] [17]. The SOM technique comprise of a two layered network that organizes the input patterns to a topological structure represented by its neurons while preserving the relations between different patterns. To achieve this, the following topology and training rules of Kohonen mapping are applied in the present study for clustering, classification, and feature extraction in MODIS spectral images from 2000 to 2014.

1) The training of the network is implemented by presenting data vectors x to the input layer of the network whose connection weight vectors m_i of all competitive neurons i are chosen random values. If N is the dimension of the satellite spectral data, we chose N input neurons and define the Euclidean distance (d_i) between x and m_i as:

$$d_i = \|x - m_i\| = \sqrt{\sum_{j=1}^N (x_j - m_{ij})^2} \tag{1}$$

and determine the activated neuron c with $d_c = \min_i \{d_i\}$.

2) Updating of the weights m_{ij} that are associated to the neurons is only performed within the proximity ($i \in N_c(t)$) of c that reduces with the training time t and $N_c(t)$ is the winning neuron. The process of updating is implemented via the Equation (2b) where $a(t)$ represents a time dependent learning rate:

$$m_{ij}^{t+1} = m_{ij}^t + \Delta m_{ij}^{(t)} \tag{2a}$$

$$\Delta m_{ij}^{(t)} = \begin{cases} a(t)(x_j - m_{ij}^{(t)}), & \text{if neuron } i \in N_c(t) \\ 0, \dots & \text{otherwise} \end{cases} \tag{2b}$$

$$a(t) = a_o \left(1 - \frac{t}{T}\right), t \in [0, \dots, T] \tag{2c}$$

The time dependent neighborhood is updated according to:

$$d(t) = d_o \left(1 - \frac{t}{T} \right), t \in [0, \dots, T] \tag{2d}$$

It is therefore important to note that the network performs two features during the training, which are strongly related to both clustering and classification of the MODIS spectral data over the region. These are:

- 1) A separation, *i.e.* cluster analysis of the presented data by mean vectors m_i that are associated as weights to the neurons.
- 2) A topological ordering of the competitive neurons in such a way that neighboring neurons in the layer represent similar clusters in multidimensional space and thus dimensionality reduction.

Based on [9], we have formulated a method that separates factors contributing to temporal change in both AOD and PR into:

- a) Portion caused by a change in the frequency of occurrence (FO) of monthly AOD and PR maps in a node.
- b) Portion due to a change in the node mean value in both AOD and PR.
- c) Portion as a result of the combination of the two effects.

The stated factors that contribute to the temporal changes in both AOD and PR, we can define the following sets of equations:

$$\Delta\tau = \sum_{i=1}^N \{ (\tau_i + \Delta\tau_i)(f_i + \Delta f_i) - \tau_i f_i \} \tag{3a}$$

$$\Delta\alpha = \sum_{i=1}^N \{ (\alpha_i + \Delta\alpha_i)(f_i + \Delta f_i) - \alpha_i f_i \} \tag{3b}$$

where $\Delta\tau$ and $\Delta\alpha$ are the total change in AOD and PR between two different time periods, τ_i and α_i are the node average variables in both AOD and PR respectively in the initial period. f_i is the FO of monthly maps in node i during the initial period while Δf_i is the change in FO for node i between the two periods of interest. Additionally, $\Delta\tau_i$ and $\Delta\alpha_i$ are the changes in both AOD and PR node average variables between the two periods while N is the total number of nodes in each SOM map over each site of study. Expanding Equation (3a) and Equation (3b), we have:

$$\Delta\tau = \sum_i^N (\tau_i \Delta f_i + f_i \Delta\tau_i + \Delta\tau_i \Delta f_i) \tag{4a}$$

$$\Delta\alpha = \sum_i^N (\alpha_i \Delta f_i + f_i \Delta\alpha_i + \Delta\alpha_i \Delta f_i) \tag{4b}$$

The first terms in Equation (4a) and Equation (4b) *i.e.* $\tau_i \Delta f_i$ and $\alpha_i \Delta f_i$ relate changes in monthly AOD and PR fields respectively to changes in the FO of aerosol optical patterns over each study site. These patterns show a portion of the total change owing to the shifts in the frequencies with which monthly AOD and PR fields reside in the patterns depicted in the SOM. A change in AOD and PR distribution represents a change in aerosol characteristics which directly and indirectly alter regional climate [18] [19] and further affect the air quality, hence, referred to as a dynamic factor. The second term in Equation (4a) and Equation (4b) *i.e.* $f_i \Delta\tau_i$ and $f_i \Delta\alpha_i$ relates the temporal evolution in AOD and PR fields respectively averaged over all months belonging to a give node. In the case of aerosol optical properties, such changes are caused by thermodynamic effects

such as local air circulation, urban heat islands effects among others. The third term in Equation (1) represents the contribution from the interaction of both changing pattern frequency and the node averaged variable for both AOD and PR. This term tends to be small as compared to the other two. For any input data matrix of n -variables (spatial variability) and m -observations (samples) (temporal variability) the iterative SOM training procedure is as detailed elsewhere [16].

3. Results and Discussions

SOM Analysis

1) Aerosol Optical Depth

SOM is normally colored by the values of the unified distance matrix (U-matrix) elements. The U-matrix is obtained according to the features of the input data and then illustrated as a component plane as displayed in **Figures 1-3** for AOD, ÅE and PR clustering. SOM performs classification of the three properties and reveals that each of the three properties essentially has at least two clusters at each site of study. From **Figure 1**, we note that each site experiences unique AOD depiction as there is no single site whose AOD variability correlates with the others in the study period. This implies the fact that AOD characteristics over the study site are highly variable. The two clusters in the AOD over each study site are attributed the two dry and wet seasons experienced over the region [21]. Additionally, the East Africa region's aerosol characteristics are modulated by the Monsoon precipitation [22]. On the contrary, Kampala is dominated by a single cluster in AOD during the study period; this may be attributed to the significant vehicular emissions [23]. Likewise, Mbita is dominated by a single AOD cluster over the study period that may be as a result of biomass burning and land preparation for agricultural use [21]. SOM AOD map for each study site is illustrated in **Figure 1**.

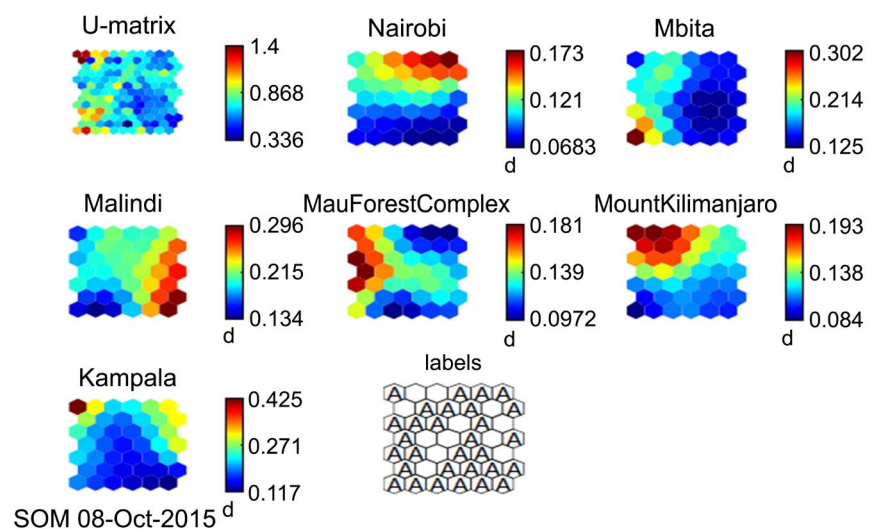


Figure 1. SOM classification of AOD over the six variables.

2) Ångström Exponent

It has been demonstrated that the ÅE is a good indicator of fraction of small aerosol particles with radii $r = 0.057 - 0.21 \mu\text{m}$ relative to large particles with radii $r = 1.8 - 4 \mu\text{m}$ for atmospheric aerosols [24]. Additionally, the ÅE is often used as a qualitative indicator of aerosol particle size, with values greater than 2 indicating small particles associated with combustion byproducts, and values less than 1 indicating large particles like sea salt and dust [25]. **Figure 2** shows the application of SOM on ÅE over each study site, specifically, Mbita and Mount Kilimanjaro are highly correlated and dominated by a single cluster. The single cluster can be attributed to the anthropogenic influence over the study sites *i.e.* land clearance, deforestation activities and biomass burning that dominate the study sites [21] [26]. This conclusion is arrived at since from **Figure 3** the two sites experience distinct precipitation rates during the study period. On the contrary, Nairobi is characterized by two clear clusters attributed to dry and wet seasons experienced over the site. The dominant aerosol particles over the site constitute vehicular and industrial emissions, biomass and refuse burning [27] as well as their long distance transport from the surrounding regions. These aerosol particles are highly hygroscopic in nature [28], hence, the two clear clusters that are modulated by the two seasons experienced over Nairobi. On the other hand, Kampala experienced two clusters but with relatively higher values in ÅE as compared to the rest of the study sites in the region. These values suggest the dominance of aerosol particles in the $\lambda = 670 \text{ nm}$ wavelength, these aerosol particles originate from vehicular emissions [23]. Malindi displays the least values in ÅE suggesting the existence of sea spray, sea salt and long distance transport of aerosol particles from the Arabian Peninsula desert via Monsoon winds which indeed are seasonal [20]. Likewise, SOM displays two clusters over Mau Forest complex which are associated to the two prevailing seasons experienced over the site. Additionally, continual biomass burning and forest

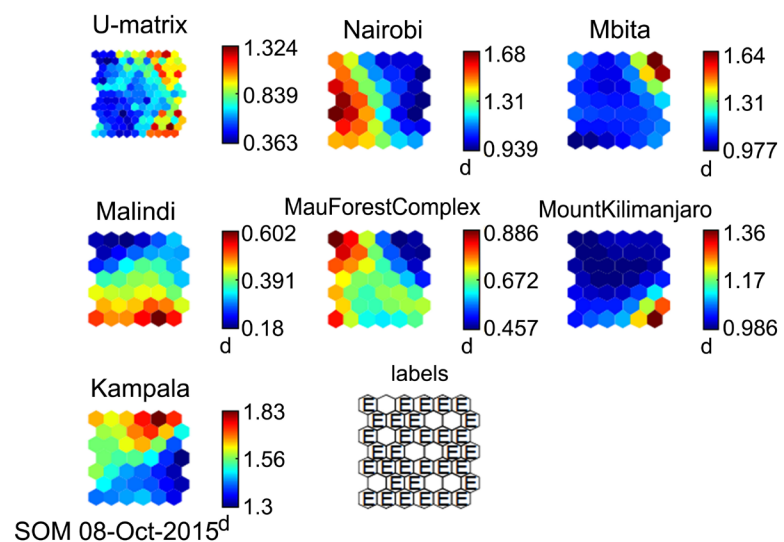


Figure 2. SOM classification of ÅE over the six variables.

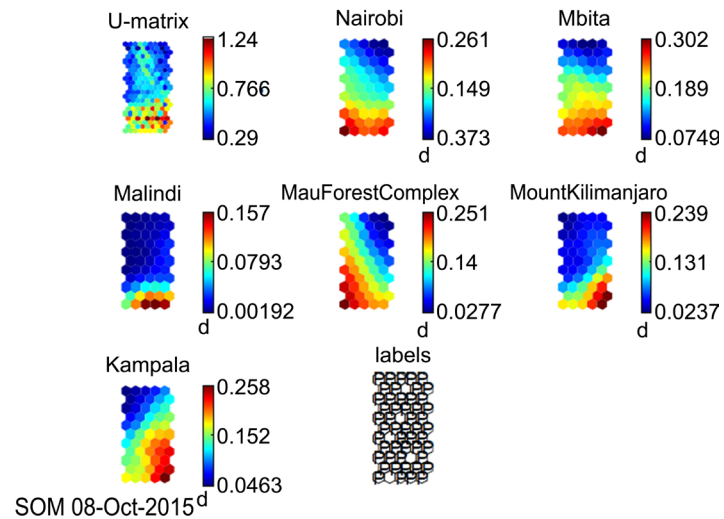


Figure 3. SOM classification of PR over the six variables.

clearance for agricultural use over Mau Forest Complex [29] [30], enhance the region's aerosol particles whose ÅE values span in the range $(0.46 - 0.89 \pm 0.07)$.

3) Precipitation Rate

From **Figure 3**, Nairobi, Mbita, Mau Forest Complex, Mount Kilimanjaro all significantly experience both dry and wet seasons during the study period. On the contrary, Malindi experiences the lowest PR as compared to the rest of the region. SOM displays two clusters over each study site that is attributed prevailing seasonal variation over the region.

4. Conclusion

MODIS Terra monthly AOD and ÅE level 3 data from 2000 to 2014 are used to optical characterization of atmospheric aerosols using the SOM algorithm. The SOM algorithm classification of both AOD and ÅE is attributed to anthropogenic influences among them land clearance, deforestation activities and biomass burning that dominate the study sites. SOM displays two clusters over each study site except Mbita that is attributed prevailing seasonal variability in the precipitation rates over the region therefore emphasizing the role of precipitation on evaluating aerosol effects. On the contrary, a single cluster in AOD and ÅE over Mbita points towards the fact that aerosol characteristics over the site are mainly depended on both biomass burning and local air circulation rather than the monsoon precipitation throughout the study period.

Acknowledgements

This work was supported by the National Council for Science and Technology Grant funded by the Government of Kenya (NCST/ST&I/RCD/4TH call PhD/201). The authors wish to thank the NASA Goddard Earth Science Distributed Active Archive for MODIS Level 3, TRMM rainfall data which served as a complement to the meteorological data from the Kenya Meteorological Department.

Conflicts of Interest

The authors declare no conflicts of interest regarding the publication of this paper.

References

- [1] Karp, A.N., Griffin, J.L. and Kathryn, S.L. (2005) Application of Partial Least Squares Discriminant Analysis to Two-Dimensional Difference Gel Studies in Expression Proteomics. *Proteomics*, **5**, 81-90. <https://doi.org/10.1002/pmic.200400881>
- [2] Makokha, J.W., Angeyo, H.K and Muthama, J.N. (2015) Sun-Photometric Study and Multivariate Analysis of Aerosol Optical Depth Variability over Some Representative Sites of the Kenyan Atmosphere. *International Journal of Biochemistry*, **23**, 15-28.
- [3] Liu, Y. and Weisberg, R. (2005). Patterns of Ocean Current Variability on the West Florida Shelf Using the Self-Organizing Map. *Journal of Geophysical Research*, **110**, C06003. <https://doi.org/10.1029/2004JC002786>
- [4] Liu, Y. and Weisberg, R.H. (2011) A Review of Self-Organizing Map Applications in Meteorology and Oceanography, Self Organizing Maps—Applications and Novel Algorithm Design. In: Mwasiagi, J.I., Ed., InTech.
- [5] Makokha, J.W., Angeyo, H.K. and Muthama, J.N. (2017) Aerosol Optical Depth and Precipitation Projections over East Africa Utilizing Self-Organizing Map. *International Journal of Science & Technology*, **5**, 166-175.
- [6] Oja, M., Kaski, S. and Kohonen, T. (2003) Bibliography of Self-Organizing Map (SOM) Papers: 1998-2001 Addendum. *Neural Computing Surveys*, **3**, 1-156.
- [7] Hong, Y., Hsu, K., Sorooshian, S. and Gao, X. (2004) Precipitation Estimation from Remotely Sensed Imagery Using an Artificial Neural Network Cloud Classification System. *Journal of Applied Meteorology*, **43**, 1834-1853. <https://doi.org/10.1175/JAM2173.1>
- [8] Liu, Y., Weisberg, R.H. and He, R. (2006) Sea Surface Temperature Patterns on the West Florida Shelf Using the Growing Hierarchical Self-Organizing Maps. *Journal of Atmospheric and Oceanic Technology*, **23**, 325-328. <https://doi.org/10.1175/JTECH1848.1>
- [9] Cassano, J.J., Uotila, P., Lynch, A.H. and Cassano, E.N. (2007) Predicted Changes in Synoptic Forcing of Net Precipitation in Large Arctic River Basins during the 21st Century. *Journal of Geophysical Research*, **112**, G04S49. <https://doi.org/10.1029/2006JG000332>
- [10] Natasa, S. and Jennifer, F. (2012) Self-Organizing Maps: A Powerful Tool for the Atmospheric Sciences, Applications of Self-Organizing Maps. In: Johnsson, M., Ed., InTech.
- [11] Levy, R.C., Remer, L.A., Mattoo, S., Vermote, E.F. and Kaufman, Y.J. (2007) Second Generation Operational Algorithm: Retrieval of Aerosol Properties over Land from Inversion of Moderate Resolution Imaging Spectroradiometer Spectral Reflectance: New Modis Retrieval of Aerosol over Land. *Journal of Geophysical Research*, **112**, D13211. <https://doi.org/10.1029/2006JD007811>
- [12] Remer, L.A., Kleidman, R.G., Levy, R.C., Kaufman, Y.J., Tanré, D., Mattoo, S., Martins, J.V., Ichoku, C., Koren, I., Yu, H. and Holben, B.N. (2008) Global Aerosol Climatology from the MODIS Satellite Sensors. *Journal of Geophysical Research: Atmospheres*, **113**, D14S07. <https://doi.org/10.1029/2007JD009661>
- [13] Ichoku, C., Kaufman, Y.J., Remmer, L.A. and Levy R. (2004) Global Aerosol Remote

Sensing from MODIS. *Advances in Space Research*, **34**, 820-827.

<https://doi.org/10.1016/j.asr.2003.07.071>

- [14] Simpson, J.S., Kummerow, C., Tao, W.K. and Adler, R.F. (1996) On the Tropical Rainfall Measuring Mission (TRMM). *Meteorology and Atmospheric Physics*, **60**, 19-36. <https://doi.org/10.1007/BF01029783>
- [15] Makokha, J.W., Odhiambo, J.O. and Godfrey, J.S. (2017) Trend Analysis of Aerosol Optical Depth and Ångström Exponent Anomaly over East Africa. *Atmospheric and Climate Sciences*, **7**, 588-603. <https://doi.org/10.4236/acs.2017.74043>
- [16] Kohonen, T. (1982) Self-Organized Information of Topologically Correct Features Maps. *Biological Cybernetics*, **43**, 59-69. <https://doi.org/10.1007/BF00337288>
- [17] Kohonen, T. (2001) Self-Organizing Maps. Springer-Verlag, New York, Berlin, Heidelberg. <https://doi.org/10.1007/978-3-642-56927-2>
- [18] Charlson, R.J., Schwartz, S.E., Hales, J.M., Cess, R.D., Coakley, J.A., Hansen, J.E. and Hofmann, D.J. (1992) Climate Forcing by Anthropogenic Aerosols. *Science*, **255**, 423-430. <https://doi.org/10.1126/science.255.5043.423>
- [19] Intergovernmental Panel on Climate Change (IPCC) (2007) Climate Change 2007: The Specific Basis. Contribution of Working Group 1 for the Fourth Assessment Report. Assessment Report of the Intergovernmental Panel on Climate Change. Cambridge University Press, Cambridge and New York, 131-234.
- [20] Crane, R.G. and Hewitson, B.C. (2003) Clustering and Upscaling of Station Precipitation Records to Regional Patterns Using Self-Organizing Maps (SOMs). *Climate Research*, **25**, 95-107. <https://doi.org/10.3354/cr025095>
- [21] Makokha, J.W. and Angeyo, H.K. (2013) Investigation of Radiative Characteristics of the Kenyan Atmosphere Due to Aerosols Using Sun Spectrophotometry Measurements and the COART Model. *Aerosol Air Quality Research*, **13**, 201-208. <https://doi.org/10.4209/aaqr.2012.06.0146>
- [22] De Graaf, M., Tilstra, L.G., Aben, I. and Stammes, P. (2010) Satellite Observations of the Seasonal Cycles of Absorbing Aerosols in Africa Related to the Monsoon Rainfall, 1995-2008. *Atmospheric Environment*, **44**, 1274-1283. <https://doi.org/10.1016/j.atmosenv.2009.12.038>
- [23] Mabasi, T. (2009) Assessing the Impacts, Vulnerability, Mitigation, and Adaptation to Climate Change in Kampala City. *5th Urban Research Symposium, Marseille*, 28-30 June 2009, 1-15.
- [24] Kaufman, Y.J., Tanré, D., Gordon, H.R., Nakajima, T., Lenoble, J., Frouin, R., Grassl, H., Herman, B.M., King, M.D. and Teillet, P.M. (1997) Passive Remote Sensing of Tropospheric Aerosol and Atmospheric Correction for the Aerosol Effect. *Journal of Geophysical Research*, **102**, 16815-16830. <https://doi.org/10.1029/97JD01496>
- [25] Schuster, G.L., Dubovik, O. and Holben, B.N. (2006) Angstrom Exponent and Bimodal Aerosol Size Distributions. *Journal of Geophysical Research*, **111**, D07207. <https://doi.org/10.1029/2005JD006328>
- [26] Fairman, J.G., Nair, U.S., Christopher, S.A. and Mölg, T. (2011) Land Use Change Impacts on Regional Climate over Kilimanjaro. *Journal of Geophysical Research Atmospheres*, **116**, D03110. <https://doi.org/10.1029/2010JD014712>
- [27] van Vliet, E.D.S. and Kinney, P.L. (2007) Impacts of Roadway Emissions on Urban Particulate Matter Concentrations in Sub-Saharan Africa: New Evidence from Nairobi, Kenya. *Environmental Research Letters*, **2**, Article ID: 045028. <https://doi.org/10.1088/1748-9326/2/4/045028>
- [28] Lei, T., Zuend, A., Wang, W.G., Zhang, Y.H. and Ge, M.F. (2014) Hygroscopicity of

Organic Compounds from Biomass Burning and Their Influence on the Water Uptake of Mixed Organic Ammonium Sulfate Aerosols. *Atmospheric Chemistry and Physics*, **14**, 11165-11183. <https://doi.org/10.5194/acp-14-11165-2014>

- [29] National Environmental Management Authority, Kenya (NEMA) (2013) Mau at a Glance. NEMA Report.
- [30] Mutugi, M. and Kiiru, W. (2015) Biodiversity, Local Resource, National Heritage, Regional Concern and Global Impact: The Case of Mau Forest, Kenya. *European Scientific Journal*, **1**, 681-691.